

Open Access



1 **Original Article**

2 **Furry is a component of the CCM3-GCKIII signaling pathway**

3

4 **Emmanuel Antwi-Adjei¹, Alondra S. Burguete², Amin S. Ghabrial¹**

5

6 ¹Department of Pathology and Cell Biology, Columbia University Irving Medical
7 Center, New York, NY 10032, USA.

8 ²Department of Neurology Columbia University Irving Medical Center, New York, NY
9 10032, USA.

10

11 **Correspondence to:** Prof. Amin S. Ghabrial, Department of Pathology and Cell
12 biology, Columbia University Irving Medical Center, 630 W. 168th Street, VP&S
13 14-401L, New York, NY 10032, USA. E-mail: asg2236@cumc.columbia.edu

14

15 **How to cite this article:** Antwi-Adjei E, Burguete AS, Ghabrial AS. Furry is a
16 component of the CCM3-GCKIII signaling pathway. *Vessel Plus* 2021;5:[Accept].
17 <https://dx.doi.org/10.20517/2574-1209.2021.48>

18

19 **Received:** 23 Mar 2021 **Revised:** 30 Apr 2021 **Accepted:** 26 May 2021 **First**
20 **online:** 26 May 2021

21

22 **ABSTRACT**

23 **Aim:** Mutations in 3 genes encoding proteins of the Cerebral Cavernous Malformations



© The Author(s) 2018. Open Access This article is licensed under a Creative Commons Attribution 4.0 International License (<https://creativecommons.org/licenses/by/4.0/>), which permits unrestricted use, sharing, adaptation, distribution and reproduction in any medium or format, for any purpose, even commercially, as long as you give appropriate credit to the original author(s) and the source, provide a link to the Creative Commons license, and indicate if changes were made.

24 (CCM) ternary complex, cause autosomal dominant cerebral vascular disease. Targets
25 of CCM complex regulation have been identified; however, the molecular mechanisms
26 connecting CCM3 to these downstream effectors remain elusive. We aim to determine
27 the mechanism of CCM3 action by using a *Drosophila* model to elucidate the signaling
28 pathway downstream of CCM3. Previously, we showed that CCM3 and its binding
29 partner, Germinal Center Kinase 3, are required in tracheal terminal cells to prevent
30 tube morphogenesis defects. Further, we established that GCKIII phosphorylates and
31 directly activates a downstream kinase, Tricornered (*Drosophila* STK38/38L ortholog).
32 Here we aim to test whether Tricornered-associated scaffolding protein, Furry, is
33 required for CCM3-GCKIII signaling.

34

35 **Methods:** We utilized the FRT-FLP system to generate genetic mosaic *Drosophila*
36 larvae and adults. Mitotic recombination was induced in embryos (trachea) or larvae
37 (wing disc). The animals were heterozygous for the gene of interest (*ccm3* or *furry*), but
38 after recombination, homozygous mutant daughter cells were produced. In addition, the
39 GAL4-UAS system was used to express dominant negative GCKIII in wing disc cells.
40 Mutant cells were analyzed by brightfield and/or fluorescent microscopy.

41

42 **Results:** We find that wing cells mutant for *ccm3*, or expressing dominant negative
43 GCKIII, produce wing hair defects characteristic of mutations in *tricornered* and *furry*.
44 Likewise, tracheal terminal cells mutant for *furry* produce tube dilation defects
45 characteristic of cells mutant for *ccm3* or *GCKIII*.

46

47 **Conclusion:** CCM3 and GCKIII act upstream of Furry-Tricornered, suggesting the
48 conservation from yeast of a Hippo-like signaling pathway that regulates
49 morphogenesis. We speculate that some combination of Furry/Furrylike and
50 STK38/38L are therefore likely to act downstream of CCM3 in endothelial cells.

51

52 **Keywords:** CCM3, GCKIII, NDR, STK38/38L, tube morphogenesis, planar cell
53 polarity

54

55

56 **INTRODUCTION**

57 Cerebral cavernous malformations (CCMs) are common vascular defects found in the
58 capillaries of the central nervous system (reviewed in Lampugnani et al. ^[1]). Familial
59 CCM shows an autosomal dominant manner of inheritance, with variable expression
60 and incomplete penetrance (reviewed in Riolo et al. ^[2]). Somatic loss of a second
61 (Knudsonian 2 hit mechanism) CCM allele ^[3] is believed to result in localized vascular
62 lesions in which grossly dilated, thin-walled capillaries lacking surrounding support
63 cells undergo repeated hemorrhage leading to headaches, neurological deficits and
64 stroke ^[4]. Lesions are believed to be largely clonally derived, containing few wild type
65 endothelial cells ^[5] (although also see ^[6]). Mutations in three different genes cause
66 disease and account for at least 80% of cases of familial CCM. These genes – *Krev*
67 *interaction trapped protein 1 (Krit1)*, *Malcavernin*, and *Programmed Cell Death 10*
68 *(PDCD10)* – are also known as *CCM1*, *CCM2* and *CCM3*, respectively. Generally, the
69 CCM proteins have been thought to act as scaffolding for regulators of cytoskeletal
70 remodeling and/or signaling pathways. The CCM proteins can physically interact,
71 forming a ternary complex bridged by CCM2. The complex may be recruited to the
72 plasma membrane through interaction with a putative transmembrane receptor protein,
73 Heart of Glass ^[7], or by interaction with the Vascular endothelial growth factor receptor
74 2 (VEGFR-2) ^[8, 9]. The precise functions of the individual proteins, and of the various
75 complexes, remain key subjects of inquiry. The role of CCM3 has been particularly
76 controversial, as CCM3 is also found in other complexes ^[10] and has been suggested to
77 operate in a CCM1- and CCM2-independent manner ^[11-15].

78

79 Consistent with the idea that CCM3 may act independently of CCM1 and CCM2,
80 mutations in *CCM3* cause an earlier lethality in mice, and in humans, patients with
81 *CCM3* mutations show a much earlier age of onset and a more severe course of disease
82 ^[12, 16-18]. Likewise, patients with mutations in *CCM3*, but not *CCM1* or *CCM2*, develop

83 multiple meningiomas at a high frequency ^[17]. These differences may reflect a
84 requirement for CCM3 in epithelia ^[19], or may hint at a distinct molecular function for
85 CCM3 even in endothelial cells.

86

87 We have turned to the simple *Drosophila melanogaster* model system to dissect CCM3
88 function. Importantly, CCM3 is well conserved, but neither CCM1 nor CCM2
89 orthologs have been reported in flies. In prior work, we identified a requirement for
90 CCM3 and GCKIII in tracheal terminal cell tube morphogenesis [20], and have since
91 gone on to show that GCKIII directly activates the Nuclear Dbf2-related (NDR) kinase,
92 Tricornered (NDR1, 2 in vertebrates, also known as STK38 and STK38L) by
93 phosphorylation ^[21]. Altogether, our work shows that CCM3 is a novel component of an
94 ancient kinase cascade conserved from yeast: the RAM (Regulation of Ace2 and
95 Morphogenesis) pathway in budding yeast, and the MOR (Morphogenesis Orb6
96 network) pathway in *Schizosacharomyces pombe* ^[22].

97

98 In yeast and flies, NDR kinase signaling typically requires co-factors including Mob
99 (mps one binder) and Furry family members ^[23]. Four Mob family members have
100 been identified (Mats, Mob2, Mob3 and Mob4) in flies, and single Furry protein
101 (Tao3p in budding yeast and Mor2p in fission yeast). So far work on the invertebrate
102 *fry* genes indicate essential roles in Trc signaling, with known requirements in the
103 generation of actin-based cellular protrusions (wing hairs and bristles ^[24-30]), in the
104 control of dendritic branching and tiling in dendritic arborization neurons ^[31-33], and in
105 follicle cell polarity ^[34]. The vertebrate orthologs of Fry (FRY and FRYL) have been
106 implicated in several processes ^[23], including tubulogenesis in the kidney ^[35, 36], but
107 have not yet been linked to vascular biology.

108

109 **METHODS**

110 Wings. Young adult flies (newly eclosed up to 1 day old) were anesthetized on CO₂
111 pads and then transferred into 100% ethanol in glass dissection dishes. Using

112 microdissection spring scissors and Dumont forceps (Fine Science Tools, Foster, CA,
113 USA), the wings were clipped off at their attachment site. Wings were transferred to a
114 drop of Euparal (BioQuip, 6372A), and a coverslip was applied. Weights were placed
115 on the coverslip to flatten the specimens, and slides were allowed to dry at room
116 temperature for 1 day or more before imaging. Images were captured at the wing
117 margin and just distal to the cross-vein connecting wing vein 3 and 4. For *ccm3*
118 mosaic wings, virgin FRT^{82B} *ccm3*/TM6B flies were crossed with *y, w, hsFLP¹²²*;
119 FRT^{82B} males, and the progeny (embryos and larvae) were subjected to heat shocks
120 (38.5 °C) for 1 – 2 hrs starting at 6 hrs after egg lay (a.e.l.). Heat shocks were
121 repeated every day through the end of the 3rd larval instar. Heat shock induction of
122 Flipase (FLP), a site-specific recombinase, resulted in mitotic recombination between
123 the homologous chromosomes at a centromere proximal FLP Recombinase Target (FRT)
124 site (FRT^{82B}). As a consequence, genetic mosaic animals were produced with most
125 cells being heterozygous, but with clones of homozygous wild type and homozygous
126 mutant cells. Mosaic adults were easily recognized by eye color mosaicism, as well
127 as by an unevenness of the wing surfaces (mosaic wings appeared somewhat crinkled
128 rather than the wild type flat appearance that characterized the wings of their TM6B
129 siblings). For GckIII_{T167A} wing analysis, the wing specific *nubGAL4* driver flies were
130 crossed to the UAS-GckIII_{T167A}^{F2} flies (dominant negative, non-phosphorylatable
131 GCKIII [21]).

132

133 Mosaic analysis of larval trachea. To test the cell autonomous requirement for *furry* and
134 *Mo25* in tracheal cells we generated genetic mosaic animals using FLP-FRT
135 approaches [37, 38]. The alleles *fry*^{O31}, *fry*^{O41} and *fry*^{O98} were gifts from Dr. Sally
136 Horne-Badovinac and encode truncated Fry proteins (Q1008term, W394term and
137 G666term, respectively). The *fry*¹ allele [23] carries a 1 bp deletion causing a
138 frame-shift after aa 403. Lastly, the *fry*^{s308} allele comes from an EMS/X-ray screen for
139 modifiers of *sina*GMR.PN eye phenotype [40]. Except for *fry*^{s308}, all *fry* alleles were
140 induced on chromosomes carrying FRT^{80B}. For these alleles, mosaic larvae were
141 generated using the MARCM strategy. For *fry*^{s308}, we generated recombinant

142 chromosomes carrying both the *fry* mutation and FRT^{2A}, and generated mosaic larvae
143 using a MARCM-related approach we had previously developed, substituting a GFP
144 RNAi transgene for the *Tubulin*-GAL80 transgene. For *Mo25*, the D8-2 allele was
145 used [39]. Except for analysis of *fry*^{s308}, virgins of the genotype *y, w, hsFLP122;*
146 *btl*-GAL4, UAS-GFP, UAS-DsRED2nls; *Tub*-GAL80 FRT80B were crossed to males
147 carrying *fry* mutant alleles on FRT80B chromosomes in trans to TM3Sb, Twist>GFP.
148 For the *fry*^{s308} analysis, virgins of the genotype *y, w, hsFLP122; btl*GAL4, UAS-GFP,
149 UAS-DsRED2nls; UAS-GFP RNAi FRT2A were crossed to males of the genotype
150 *fry*^{s308} FRT2A/TM3, Sb. Crosses were established with 40 virgins and 20 – 40 males.
151 After 4 hrs at 25 °C, adults were transferred to fresh vials, and the 0-4 hrs a.e.l.
152 embryos were subjected to 45 – 60 minute heat shock. The embryos were then
153 cultured for an additional 5 days at 25 °C and analyzed at the third larval instar.
154 Mosaic larvae were identified based on the presence of individual GFP expressing cells
155 in the tracheal system (marking the homozygous mutant clones). The mosaic larvae
156 were then heat killed (~ 10 seconds at 70 °C) in a drop of 50% glycerol on a slide; a
157 cover slip was added and fluorescent microscopy was used to identify mosaic animals.
158 Mutant terminal cells were analyzed by brightfield microscopy to score the presence
159 and shape of gas-filled tubes. Cells were also analyzed by fluorescent microscopy,
160 with the black space in GFP labeled cells revealing tube lumens, including the lumens
161 of tubes that were not gas-filled (and thus not detectable by brightfield microscopy).
162 Larvae were examined using 20X and 40X objectives on a Leica compound fluorescent
163 microscope. Z-stacks were captured for each GFP positive terminal cell using Leica
164 software. Unidentified images were then scored independently for the presence of
165 transition zone tube dilations and other defects. In some instances, the position of the
166 terminal cell within the specimen did not allow analysis, these cells were excluded
167 from counts.

168

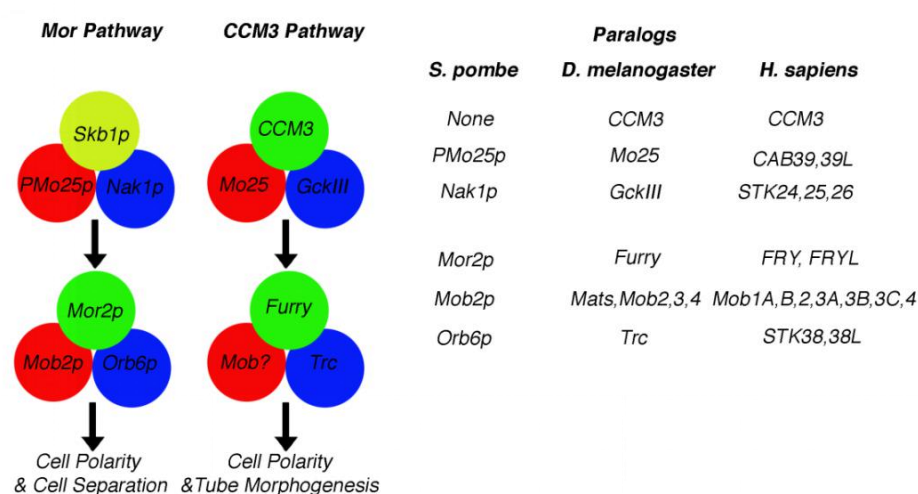
169 Microscopy. Larvae were imaged using direct fluorescence and Brightfield optics using
170 a Leica DM5500 B upright widefield epifluorescence microscope (Leica

171 Microsystems). Images were acquired using a Leica DFC360FX camera. Z-stacks
 172 were captured and processed by deconvolution using Leica Advanced Fluorescence
 173 Application Suite (Leica Microsystems). For wing hairs, wings mounted in Euparal
 174 were examined with brightfield optics using a Leica DM6000 inverted microscope, and
 175 images were captured using a Hamamatsu Orca-R2 Digital CCD camera (C10600,
 176 Hamamatsu Photonics).

177

178 RESULTS

179 We previously identified a requirement for the CCM3-GCKIII signaling pathway in the
 180 *Drosophila* tracheal system [20]. Importantly the CCM3-GCKIII tube morphogenesis
 181 program shares common components with an orthologous pathway in the human
 182 vascular system (reviewed in Riolo et al. [2]), that is partially conserved from yeast
 183 (**Figure 1**). Prior to our work, Tricornered (Trc), the most downstream kinase in the
 184 cascade, was best known for its role in the morphogenesis of other tissues [28, 31, 40].
 185 We decided to test whether regulation of Trc by CCM3-GCKIII was tissue-specific, or
 186 instead might be a general feature of Trc regulation. To do so, we turned to the
 187 *Drosophila* wing, a system widely used for studying developmental signaling pathways
 188 and planar cell polarity [41-46].



189

190 **Figure 1: CCM3 is a novel regulator of a conserved Hippo-like signaling**
 191 **pathway.** The fission yeast Morphogenesis (Mor) pathway is defined by a short

192 kinase cascade consisting of a Sterile20-like kinase (Nak1p) that phosphorylates and
193 activates an NDR kinase (Orb6p) which in turn phosphorylates effectors required for
194 cell polarity and separation [47]. Many of the proteins in this pathway are conserved
195 among eukaryotes, with CCM3 representing a novel scaffolding protein, not present in
196 yeast, for the upstream kinase complex. CCM3 binds directly to GCKIII in human,
197 zebrafish and flies [12, 48, 49]. Likewise, Mo25 can bind directly with Sterile20-like
198 kinases including GCKIII family members^[50]. Direct interactions between CCM3 and
199 Mo25 have yet to be reported.

200

201 **CCM3-GCKIII pathway regulates wing hair morphogenesis.**

202

203 In flies, wing epithelia possess planar polarity that is easily read out in each cell by the
204 position and orientation of actin-based cellular protrusions called wing hairs. In wild
205 type wing epithelial cells, a single hair that tapers to a point extends from the posterior
206 vertex of the cell, points distally, and is aligned with the hairs of neighboring cells
207 (**Figure 2A**). In *tricornered* and *furry* mutant cells, the organization of the actin-based
208 hairs appears to be disrupted such that the hairs split, giving rise to multiple hairs
209 (**Figure 2B, E**) and/or hairs with split ends [24, 28]. Although prior studies suggest no
210 role for Mo25 in wing hair morphogenesis [30], we decided to determine if disruption of
211 *ccm3* and *GckIII* activity would give rise to wing hair defects characteristic of *trc-fry* [26,
212 27], we examined wings expressing a dominant negative GCKIII isoform (**Figure 2C, F**,
213 *Gck*_{T167A} [21]), as well as *ccm3* mosaic wings (**Figure 2G**). In both cases, we found
214 that the affected wing cells developed multiple wing hairs with disruption of hair
215 orientation.

216

217

218

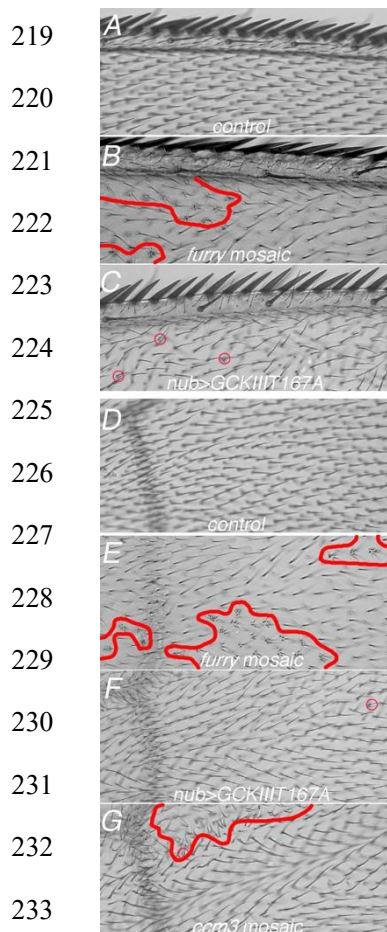


Figure 2: Like mutations in *furry*, loss of CCM3 or GCKIII

function cause wing hair number and polarity defects.

A. Anterior wing margin of a control wild type (OR-R) fly is

shown. Note that individual wing hairs are aligned, and point

towards the distal wing tip (to the right). In flies mosaic for

furry (border between cells in the mutant clone and wild type

cells outlined in red) (B), or expressing a dominant negative

(non-phosphorylatable) GCKIII isoform (GCKIII_{T167A}) (C),

orientation of the wing hairs is disrupted and (red circles) two

or more wing hairs per cell may be produced. D. Wild type

wing hairs in the area immediately proximal to the crossvein

connecting veins 3 and 4 (dark pigmentation running vertically

on the left of image) are shown. Note the presence of single

wing hairs per cell that are oriented towards the distal wing tip (right). In *furry* clones

(E) (clone borders marked in red), or wing cells expressing a dominant negative

(non-phosphorylatable) GCKIII isoform (F, GCKIII_{T167A}), orientation of the wing hairs

is disrupted and (red circles) two or more wing hairs per cell are produced. G. In wings

that are mosaic for loss of *ccm3* function (clone outlined in red), mutant cells produce

multiple wing hairs and display altered orientation. We note that in addition to the

number of wing hairs per cell, mutations in the CCM3/GCKIII-Trc/Fry pathway may

also affect planar cell polarity such that the orientation of the hairs appear perturbed.

Scale bar in G (for A-G) = 10 microns.

Furry is required in tracheal terminal cell tube morphogenesis

Furry has been identified genetically and biochemically as a partner for Trc [24, 26, 27],

and has been shown to function together with Trc in the shaping of actin-based cellular

projections (wing hairs, etc.) in epithelial cells, as well as the polarized deposition of

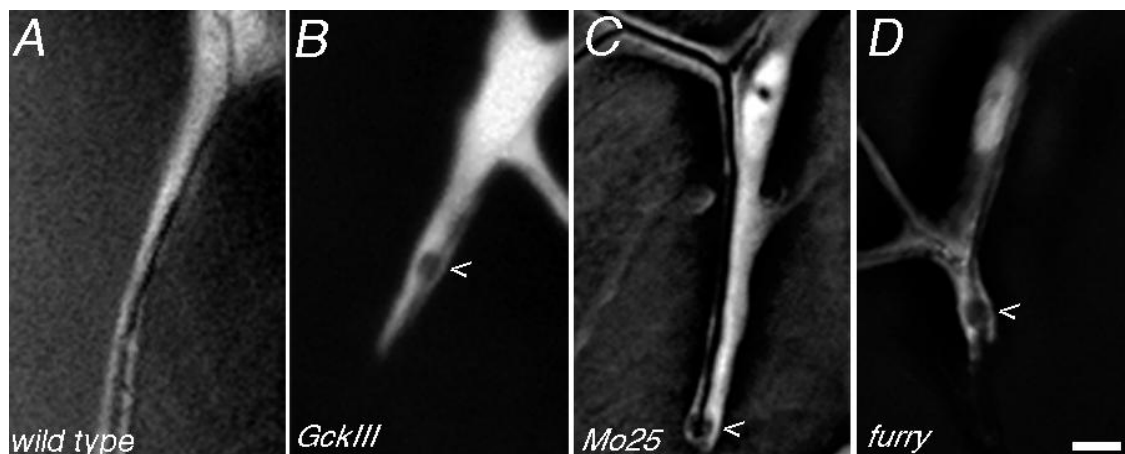
basement membrane [23]. In neurons, Fry has been shown to function with Trc in the

249 morphogenesis of dendrites [31]. A role for Fry in tubulogenesis has not been
250 examined, although *fryl* mutants in mice have been reported to have kidney defects
251 attributed to a role in the regulation of a microRNA [35, 36]. Because Furry appears to
252 be required in all other contexts where Trc function has been described as necessary for
253 morphogenesis, we tested if *furry* was also required in the tracheal system. For this
254 analysis we characterized the tracheal terminal cell phenotype of 5 independent mutant
255 alleles of *furry*, derived from 3 different genetic screens [25, 34, 51].

256

257 As has been the case for other genes in the pathway (*tao*, *ccm3*, *GckII*^[20, 21]); **Figure 3**
258 **A,B**), and is also true for *Mo25* (**Figure 3 C**) zygotic loss of *fry* appeared to uniquely
259 disrupt tube morphogenesis in terminal cells, but not other tracheal cell subtypes. In
260 homozygous *fry* terminal cells (**Figure 3 D**), we observed a range of phenotypes,
261 running from cells with tubes indistinguishable from wild type, to cells with multiple
262 transition zone dilations. The penetrance of the dilation defects varied from allele to
263 allele, with the *fry*^{s308} allele showing the most penetrant phenotype (~80%, 25/31 cells
264 showing clear transition zone dilations). In addition to transition zone tube dilations,
265 less prominent tube dilations throughout the terminal cells were also observed,
266 consistent with our prior results for other pathway members. In addition, we observed
267 gas-filling defects and melanization of the transition zone dilation – these defects were
268 less common, with lack of gas-filling observed in about 5% of mutant cells and
269 melanization in about 2% of mutant cells (n = 183 cells scored). All of these defects
270 were also described for *tricornered* mutant terminal cells^[21], and none were observed in
271 wild type control larvae, or in the heterozygous terminal cells in *fry* mosaic larvae (n =
272 50 and 50, respectively). The incomplete penetrance of the *fry* phenotype may
273 indicate a less stringent requirement for *fry* than for *GckIII* and *trc*, or may reflect the
274 presence of maternally supplied *fry* mRNA and/or protein.

275



276

277 **Figure 3: Like mutations in known CCM3-GCKIII signaling pathway**
278 **components, *furry* and *Mo25* loss of function result in tube dilations in tracheal**
279 **terminal cells.** A. The most proximal part of a wild type control terminal cell clone
280 (GFP positive labeling of homozygous cells) is shown, depicting the portion of the
281 terminal cell that extends from its intercellular junction with a neighboring stalk cell, at
282 the bottom of the image, to the terminal cell nucleus, at the top of image). In wild type
283 cells the lumen tapers very gradually and evenly from proximal (bottom) to distal (top).
284 B. In *wheezy/GckIII* mutant terminal cells, prominent transition zone (between
285 intercellular junction and terminal cell nucleus) dilations are detected (<). Terminal
286 cells mutant or knocked down for *tao*, *ccm3*, *trc* (not shown, see ^[20, 21]), (C) *Mo25*, or
287 (D) *furry* show identical transition zone dilations. Scale bar = 10 microns.

288

289 DISCUSSION

290 The molecular mechanisms by which CCM3 acts in the vascular system remain unclear.
291 Strong data support a role of GCKIII family kinases acting together with CCM3, but
292 the downstream target(s) of the kinase have remained elusive. Our prior work in
293 *Drosophila* ^[21] suggest that the NDR kinases (Trc in flies, STK38, STK38L in human)
294 are likely to be the direct targets of the CCM3/GCKIII complex in endothelial cells.
295 Studies linking the scaffolding protein Furry to Trc function implied that Furry was also
296 likely to be required as part of the CCM3-GCKIII signaling cascade. Here we
297 establish that at least in the fly tracheal system, the Furry/Trc complex is regulated by
298 CCM3/GCKIII. The connection between the CCM3-GCKIII complex and a

299 Trc-Fry-Mob complex was suggested by *in vitro* work using human orthologs [52, 53];
300 however, other factors such as mTor or Hippo have also been proposed to act as
301 upstream activators of Trc [32, 33, 40, 54]. Our data in the *Drosophila* wing demonstrate
302 that at least in two tissues, wing and trachea, Fry/Trc are regulated by the CCM3
303 pathway. Further studies in additional Trc-requiring tissues, such as neurons and
304 follicle cell epithelia, will need to be carried to determine whether the CCM3 pathway
305 is a tissue-specific or general regulator of Fry/Trc activity. Likewise, it will be critical
306 to extend the analysis to the vertebrate vascular system. If STK38 and STK38L are
307 required downstream of CCM3 in endothelial cells, as expected, it will be important to
308 identify the targets of STK38 and STK38L kinases and to determine if they are
309 universal, differ between epithelial and neural tissues, or show even greater specificity.
310 Given the role for CCM3-GCKIII in Trc-regulated tissue polarity in the wing, it will
311 likewise be of interest to gain mechanistic insight into that process, and to determine
312 whether such functions of CCM3 are related to meningiomas associated with CCM3
313 patients. The hypothesis that planar cell polarity (PCP) might be disturbed in
314 meningiomas arises from the observation that a histological characteristic of
315 meningiomas is the whorl formation of neoplastic arachnoid cells. This hypothesis has
316 received some genetic support, as human *FAT2*, an ortholog of the *Drosophila* PCP
317 pathway component *Fat*, has been implicated in meningioma [55]. Moreover, *Fat*
318 protocadherens of the have been implicated in Hippo signaling [56]. In the fly, work
319 from Horne-Badovinac and colleagues revealed that *Fat2*, Fry and Trc are required to
320 polarize the follicle cell epithelia that surround the *Drosophila* oocyte. While a role
321 for CCM3-GCKIII in the follicle cells has not yet been described, it is noteworthy that
322 in these cells Trc was found to be distributed in a planar polarized fashion. Strikingly,
323 it was the basolateral aspect of the cells that displayed these asymmetries in Trc
324 distribution, raising the question of whether the mechanisms involved are related to the
325 canonical PCP pathways, or novel.

326

327

328 **DECLARATIONS**

329 **Authors' contributions**

330 ASB and ASG made substantial contributions to conception and design of the study and
331 EA-A, ASB, and ASG performed data analysis and interpretation.

332

333 **Availability of data and materials**

334 All reagents developed in the lab are available upon request.

335

336 **Financial support and sponsorship**

337 This work was supported by NIH R01GM089782 to ASG.

338

339 **Conflicts of interest**

340 All authors declared that there are no conflicts of interest.

341

342 **Ethical approval and consent to participate**

343 Not applicable.

344

345 **Consent for publication**

346 Not applicable.

347

348 **Copyright**

349 © The Author(s) 2021.

350 **REFERENCES**

- 351 1. Lampugnani, M.G., et al., Endothelial cell disease: emerging knowledge from
352 cerebral cavernous malformations. *Curr Opin Hematol*, 2017. **24**(3): p. 256-264.

- 353 2. Riolo, G., C. Ricci, and S. Battistini, Molecular Genetic Features of Cerebral
354 Cavernous Malformations (CCM) Patients: An Overall View from Genes to
355 Endothelial Cells. *Cells*, 2021. **10**(3).
- 356 3. Pagenstecher, A., et al., A two-hit mechanism causes cerebral cavernous
357 malformations: complete inactivation of CCM1, CCM2 or CCM3 in affected
358 endothelial cells. *Hum Mol Genet*, 2009. **18**(5): p. 911-8.
- 359 4. Haasdijk, R.A., et al., Cerebral cavernous malformations: from molecular
360 pathogenesis to genetic counselling and clinical management. *Eur J Hum Genet*,
361 2011.
- 362 5. Detter, M.R., D.A. Snellings, and D.A. Marchuk, Cerebral Cavernous
363 Malformations Develop Through Clonal Expansion of Mutant Endothelial Cells.
364 *Circ Res*, 2018. **123**(10): p. 1143-1151.
- 365 6. Malinverno, M., et al., Endothelial cell clonal expansion in the development of
366 cerebral cavernous malformations. *Nat Commun*, 2019. **10**(1): p. 2761.
- 367 7. Kleaveland, B., et al., Regulation of cardiovascular development and integrity
368 by the heart of glass-cerebral cavernous malformation protein pathway. *Nat*
369 *Med*, 2009. **15**(2): p. 169-76.
- 370 8. Kean, M.J., et al., Structure-function analysis of core STRIPAK Proteins: a
371 signaling complex implicated in Golgi polarization. *J Biol Chem*, 2011. **286**(28):
372 p. 25065-75.
- 373 9. Preisinger, C., et al., YSK1 is activated by the Golgi matrix protein GM130 and
374 plays a role in cell migration through its substrate 14-3-3zeta. *J Cell Biol*, 2004.
375 **164**(7): p. 1009-20.
- 376 10. Fidalgo, M., et al., CCM3/PDCD10 stabilizes GCKIII proteins to promote
377 Golgi assembly and cell orientation. *J Cell Sci*, 2010. **123**(Pt 8): p. 1274-84.
- 378 11. Yoruk, B., et al., Ccm3 functions in a manner distinct from Ccm1 and Ccm2 in
379 a zebrafish model of CCM vascular disease. *Dev Biol*, 2012. **362**(2): p. 121-31.
- 380 12. Chan, A.C., et al., Mutations in 2 distinct genetic pathways result in cerebral
381 cavernous malformations in mice. *J Clin Invest*, 2011. **121**(5): p. 1871-81.

- 382 13. Zhu, Y., et al., Differential angiogenesis function of CCM2 and CCM3 in
383 cerebral cavernous malformations. *Neurosurg Focus*, 2010. **29**(3): p. E1.
- 384 14. Jenny Zhou, H., et al., Endothelial exocytosis of angiopoietin-2 resulting from
385 CCM3 deficiency contributes to cerebral cavernous malformation. *Nat Med*,
386 2016. **22**(9): p. 1033-1042.
- 387 15. Zhang, Y., et al., A network of interactions enables CCM3 and STK24 to
388 coordinate UNC13D-driven vesicle exocytosis in neutrophils. *Dev Cell*, 2013.
389 **27**(2): p. 215-226.
- 390 16. Denier, C., et al., Genotype-phenotype correlations in cerebral cavernous
391 malformations patients. *Ann Neurol*, 2006. **60**(5): p. 550-6.
- 392 17. Riant, F., et al., CCM3 Mutations Are Associated with Early-Onset Cerebral
393 Hemorrhage and Multiple Meningiomas. *Mol Syndromol*, 2013. **4**(4): p.
394 165-72.
- 395 18. Shenkar, R., et al., Exceptional aggressiveness of cerebral cavernous
396 malformation disease associated with PDCD10 mutations. *Genet Med*, 2015.
397 **17**(3): p. 188-196.
- 398 19. Tang, A.T., et al., Distinct cellular roles for PDCD10 define a gut-brain axis in
399 cerebral cavernous malformation. *Sci Transl Med*, 2019. **11**(520).
- 400 20. Song, Y., M. Eng, and A.S. Ghabrial, Focal defects in single-celled tubes
401 mutant for Cerebral cavernous malformation 3, GCKIII, or NSF2. *Dev Cell*,
402 2013. **25**(5): p. 507-19.
- 403 21. Poon, C.L.C., et al., A Hippo-like signalling pathway controls tracheal
404 morphogenesis in *Drosophila melanogaster*. *Dev Cell*, 2018. **47**: p. 1-12.
- 405 22. Maerz, S. and S. Seiler, Tales of RAM and MOR: NDR kinase signaling in
406 fungal morphogenesis. *Curr Opin Microbiol*, 2010. **13**(6): p. 663-71.
- 407 23. Nagai, T. and K. Mizuno, Multifaceted roles of Furry proteins in invertebrates
408 and vertebrates. *J Biochem*, 2014. **155**(3): p. 137-46.
- 409 24. He, Y., et al., The tricornered Ser/Thr protein kinase is regulated by
410 phosphorylation and interacts with furry during *Drosophila* wing hair
411 development. *Mol Biol Cell*, 2005. **16**(2): p. 689-700.

- 412 25. Cong, J., et al., The furry gene of *Drosophila* is important for maintaining the
413 integrity of cellular extensions during morphogenesis. *Development*, 2001.
414 **128**(14): p. 2793-802.
- 415 26. Fang, X. and P.N. Adler, Regulation of cell shape, wing hair initiation and the
416 actin cytoskeleton by Trc/Fry and Wts/Mats complexes. *Dev Biol*, 2010. **341**(2):
417 p. 360-74.
- 418 27. Fang, X., et al., The *Drosophila* Fry protein interacts with Trc and is highly
419 mobile in vivo. *BMC Dev Biol*, 2010. **10**: p. 40.
- 420 28. Geng, W., et al., The tricornered gene, which is required for the integrity of
421 epidermal cell extensions, encodes the *Drosophila* nuclear DBF2-related kinase.
422 *Genetics*, 2000. **156**(4): p. 1817-28.
- 423 29. He, B. and P.N. Adler, The genetic control of arista lateral morphogenesis in
424 *Drosophila*. *Dev Genes Evol*, 2002. **212**(5): p. 218-29.
- 425 30. He, Y., et al., *Drosophila* Mob family proteins interact with the related
426 tricornered (Trc) and warts (Wts) kinases. *Mol Biol Cell*, 2005. **16**(9): p.
427 4139-52.
- 428 31. Emoto, K., et al., Control of dendritic branching and tiling by the
429 Tricornered-kinase/Furry signaling pathway in *Drosophila* sensory neurons.
430 *Cell*, 2004. **119**(2): p. 245-56.
- 431 32. Emoto, K., et al., The tumour suppressor Hippo acts with the NDR kinases in
432 dendritic tiling and maintenance. *Nature*, 2006. **443**(7108): p. 210-3.
- 433 33. Koike-Kumagai, M., et al., The target of rapamycin complex 2 controls
434 dendritic tiling of *Drosophila* sensory neurons through the Tricornered kinase
435 signalling pathway. *EMBO J*, 2009. **28**(24): p. 3879-92.
- 436 34. Horne-Badovinac, S., et al., A screen for round egg mutants in *Drosophila*
437 identifies tricornered, furry, and misshapen as regulators of egg chamber
438 elongation. *G3 (Bethesda)*, 2012. **2**(3): p. 371-8.

- 439 35. Byun, Y.S., et al., Fryl deficiency is associated with defective kidney
440 development and function in mice. *Exp Biol Med* (Maywood), 2018. **243**(5): p.
441 408-417.
- 442 36. Espiritu, E.B., et al., The Lhx1-Ldb1 complex interacts with Furry to regulate
443 microRNA expression during pronephric kidney development. *Sci Rep*, 2018.
444 **8**(1): p. 16029.
- 445 37. Lee, T. and L. Luo, Mosaic analysis with a repressible cell marker for studies of
446 gene function in neuronal morphogenesis. *Neuron*, 1999. **22**(3): p. 451-61.
- 447 38. Ghabrial, A.S., B.P. Levi, and M.A. Krasnow, A systematic screen for tube
448 morphogenesis and branching genes in the *Drosophila* tracheal system. *PLoS*
449 *Genet*, 2011. **7**(7): p. e1002087.
- 450 39. Yamamoto, Y., Y. Izumi, and F. Matsuzaki, The GC kinase Fray and Mo25
451 regulate *Drosophila* asymmetric divisions. *Biochem Biophys Res Commun*,
452 2008. **366**(1): p. 212-8.
- 453 40. Natarajan, R., et al., Tricornered Kinase Regulates Synapse Development by
454 Regulating the Levels of Wiskott-Aldrich Syndrome Protein. *PLoS One*, 2015.
455 **10**(9): p. e0138188.
- 456 41. Peng, Y. and J.D. Axelrod, Asymmetric protein localization in planar cell
457 polarity: mechanisms, puzzles, and challenges. *Curr Top Dev Biol*, 2012. **101**: p.
458 33-53.
- 459 42. Strutt, H. and D. Strutt, How do the Fat-Dachsous and core planar polarity
460 pathways act together and independently to coordinate polarized cell behaviours?
461 *Open Biol*, 2021. **11**(2): p. 200356.
- 462 43. Adler, P.N., The frizzled/stan pathway and planar cell polarity in the *Drosophila*
463 wing. *Curr Top Dev Biol*, 2012. **101**: p. 1-31.
- 464 44. Bier, E., Drawing lines in the *Drosophila* wing: initiation of wing vein
465 development. *Curr Opin Genet Dev*, 2000. **10**(4): p. 393-8.
- 466 45. Matsuda, S., S. Harmansa, and M. Affolter, BMP morphogen gradients in flies.
467 *Cytokine Growth Factor Rev*, 2016. **27**: p. 119-27.

- 468 46. Swarup, S. and E.M. Verheyen, Wnt/Wingless signaling in *Drosophila*. *Cold*
469 *Spring Harb Perspect Biol*, 2012. **4**(6).
- 470 47. Gupta, S. and D. McCollum, Crosstalk between NDR kinase pathways
471 coordinates cell cycle dependent actin rearrangements. *Cell Div*, 2011. **6**: p. 19.
- 472 48. Voss, K., et al., CCM3 interacts with CCM2 indicating common pathogenesis
473 for cerebral cavernous malformations. *Neurogenetics*, 2007. **8**(4): p. 249-56.
- 474 49. Voss, K., et al., Functional analyses of human and zebrafish 18-amino acid
475 in-frame deletion pave the way for domain mapping of the cerebral cavernous
476 malformation 3 protein. *Hum Mutat*, 2009. **30**(6): p. 1003-11.
- 477 50. Filippi, B.M., et al., MO25 is a master regulator of SPAK/OSR1 and
478 MST3/MST4/YSK1 protein kinases. *EMBO J*, 2011. **30**(9): p. 1730-41.
- 479 51. Neufeld, T.P., A.H. Tang, and G.M. Rubin, A genetic screen to identify
480 components of the sina signaling pathway in *Drosophila* eye development.
481 *Genetics*, 1998. **148**(1): p. 277-86.
- 482 52. Avruch, J., et al., Protein kinases of the Hippo pathway: regulation and
483 substrates. *Semin Cell Dev Biol*, 2012. **23**(7): p. 770-84.
- 484 53. Gundogdu, R. and A. Hergovich, MOB (Mps one Binder) Proteins in the Hippo
485 Pathway and Cancer. *Cells*, 2019. **8**(6).
- 486 54. Wu, Z., et al., Tricornered/NDR kinase signaling mediates PINK1-directed
487 mitochondrial quality control and tissue maintenance. *Genes Dev*, 2013. **27**(2):
488 p. 157-62.
- 489 55. Tate, G., K. Kishimoto, and T. Mitsuya, A novel mutation of the FAT2 gene in
490 spinal meningioma. *Oncol Lett*, 2016. **12**(5): p. 3393-3396.
- 491 56. Peng, Z., Y. Gong, and X. Liang, Role of FAT1 in health and disease. *Oncol*
492 *Lett*, 2021. **21**(5): p. 398.

493